What Methanol Masers tell us about High-Mass Star Formation

Michele R. Pestalozzi
University of Hertfodshire, College Lane, AL10 9AB Hatfield, UK , michele.pestalozzi@gmail.com

with A. Chrysostomou & J. Collett (Univ. of Herts, UK), E. Elitzur (Univ. of KY, USA), J. Conway (OSO, Sweden), V. Minier (SACLAY, Paris), R. Booth (Hart'sthoek, South Africa)

1. Introduction

The galactic maser emission of methanol appears to be exclusively associated with sites of high-mass star formation (e.g. Minier et al. 2003), making them the ideal targets for both statistical and detailed study of young high-mass protostellar objects. In particular, the class II masers at 6.7 and 12.2 GHz are among the brightest masers in the Milky Way. Since their discovery, a number of extended searches have been put into action with the aim of gathering a potentially large number of objects to be studied in depth. The census of 6.7 GHz masers in the Milky Way counts to date some 520 sources, all potentially locating a high-mass protostar (Pestalozzi et al. 2005). This number is subject to increase as the Methanol MultiBeam Survey covers more regions of the galactic plane (see http://www.e-merlin.ac.uk/research/methanol/). The distribution of the known methanol masers in the Galaxy is shown in Fig. 1. Research connected with methanol masers can be summarised and organised as shown in Table 1. In this poster I will concentrate on the upper row of Table 1 and present one example for each square. In particular I will concentrate in the extraction of the luminosity function of the masers (left column) and on the recognition of a unique signature for an edge-on rotating disc marked by maser emission (right column).

	"Global" Studies	Particular Studies
Masers	**Maser luminosity** Structure of the MW Maser mechanism	**NGC7538: disc signature** Location of new sources Proper motion
Hosts of masers	Associations SEDs Follow-up obs.	IRAS20126, S255 Protoclusters

Table 1: Conceptual division of the study of methanol masers. This posters presents examples of the studies highlighted in red: Maser luminosity in the left column, disc signature in the right.

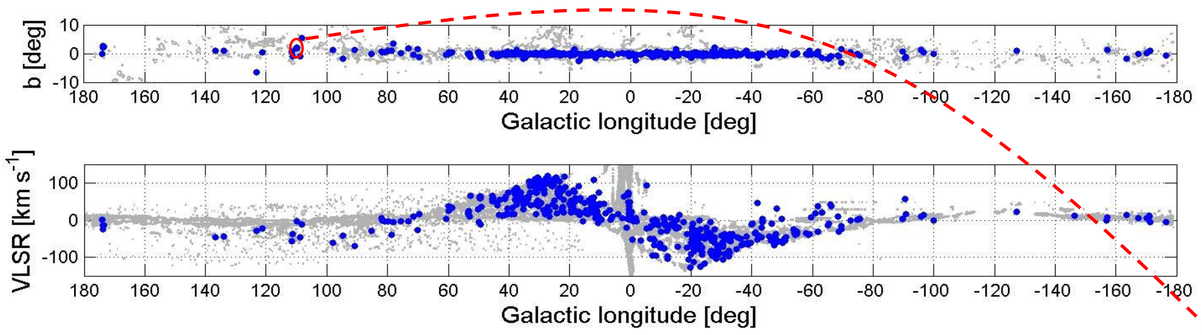

Figure 1: Distribution of 6.7GHz methanol masers in the Milky Way superposed on CO contours from Dame et al. 1897, in space (top) and LOS velocity (bottom). Methanol masers seem to accurately follow both the morphological and dynamical structure of the Galaxy. Particularly visible in the bottom panel is that methanol masers are tracing the spiral arms ($150^0 < l < 50^0$) and $-40^0 < l < -90^0$) and the high rotation velocity in the nuclear ring ($l \sim 0^0$).

2. Luminosity function of 6.7GHz methanol masers

The following figures illustrate the procedure and assumptions used to obtain an estimate of the luminosity function of methanol masers. **The luminosity function of 6.7GHz methanol masers can be modelled as a single power-law with sharp cutoffs at 10^{-8} and 10^{-3} $L_\odot$ and index between -2 and -1.5.**

Starting point for the modelling is the galactocentric distribution of sources as shown in Fig.2. The profile of the distribution *F(R)* is applied to the entire Galaxy and multiplied with an intrinsic luminosity function *N(L)* modelled with a single power-law between sharp cutoffs (assumed to enclose all methanol masers) L_{min} and L_{max} and index p. The obtained function *FxN* is "observed" at a certain sensitivity (Fig. 3) and the *observed* luminosity distribution of methanol masers in the Galaxy is produced and compared with the data (Fig.4). The free parameters in the model are the real total number of sources in the Galaxy and the index of the luminosity function. An example is shown by the blue stars in Fig. 4.

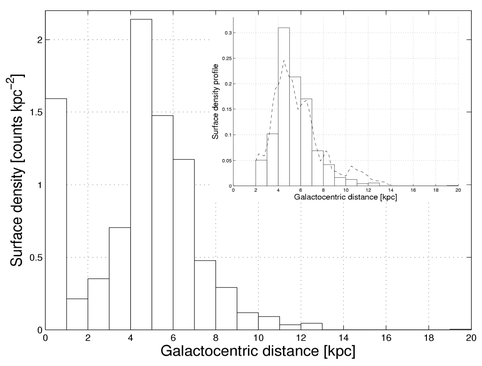

Figure 2: Surface density of the known methanol masers in galactocentric distance. The distribution shows a peak at the same radius than OB associations. The inset shows a comparison of the surface density of the masers with the molecular gas in the Milky Way. This is the starting point of the study of the luminosity function of methanol masers in the MW. The shape of he profile is considered to be real, allowing to separate spatial distribution from intrinsic luminosity distribution.

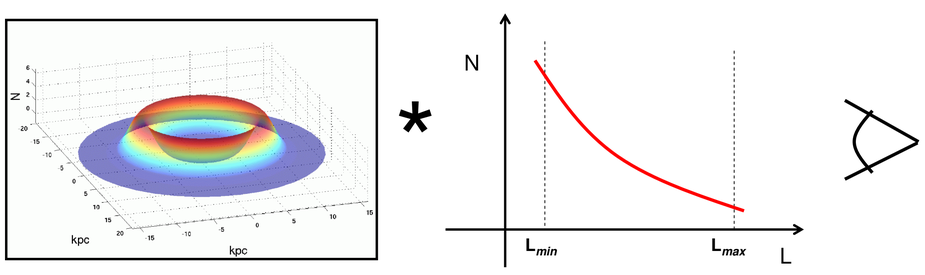

Figure 3: Graphical representation of the model used to study the luminosity function of 6.7GHz methanol masers in the Galaxy. The profile in Fig. 2 is extruded to the entire Galaxy, multiplied with a (intrinsic!) luminosity function and then observed at a certain sensitivity. Considering the spatial distribution of sources in the Galaxy to be reliable in shape, the unknowns of the problem are the total number of sources in the Galaxy and the index of the luminosity. The sharp cutoffs L_{min} and L_{max} are assumed to soan over the real range of maser luminosities.

Figure 4: Comparison between modelled luminosity distribution and observations. Dots and diamonds show the luminosity distribution of methanol masers when considering the ambiguous sources at the near- or far heliocentric distance, respectively. Blue stars show the luminosity distribution of 2000 sources with a spatial distribution as in Fig. 2 and luminosity function with index -1.7, observed with a sensitivity of 2Jy. The total number of sources found here is consitient with other estimates (e.g. van der Walt 2005).

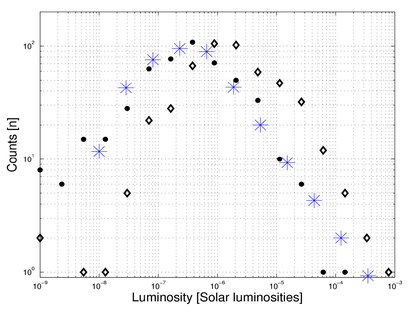

References: Pestalozzi et al. 2004, ApJ, 603, L113; Pestalozzi et al. 2005, A&A, 432, 737; Pestalozzi et al. 2006, A&A, 448, L57; Pestalozzi et al. 2007, A&A, 463, 1009; Minier et al. 1998, A&A, 336, L5; Minier et al. 2003, A&A, 403, 1095; van der Walt 2005, MNRAS, 360, 153; Dame et al. 1987, ApJ, 322,706

3. A differentially rotating disc seen edge-on

We model the optical depth of a rotating disc seen edge-on (data in Fig. 5) as equal to the length of velocity coherent paths weighted by the distribution of the masing material (Fig. 6). The final fit has three free parameters: the rotation velocity at some reference radius, the index characterising the weighting function η and the index of the rotation curve. We conclude that **the data show features that are unambiguous for differential rotation**: a maximum in the centre in space and LOS velocity, and a clear bend of the gradient at displacements outside the bulk of the emission, as shown in Fig. 7 (in our case < 20mas). The central mass is estimated to be at least 13 $M_\odot$, and the peak of the function η to be at a radius of 100mas, or about 270AU, at the distance of NGC7538 (Fig. 8).

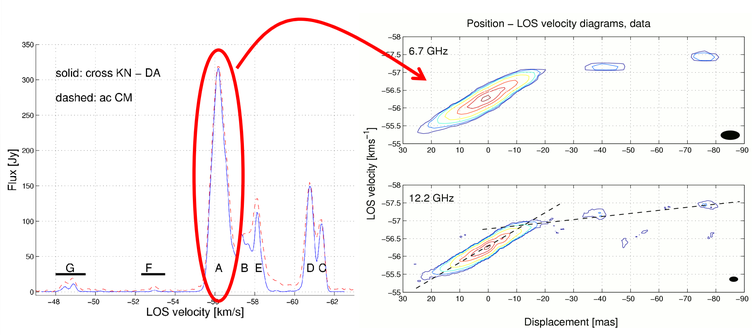

Figure 5: Left: spectrum of the 6.7GHz methanol maser emission towards NGC7538 IRS1 N. Notice that the 12.2GHz is similar in the features A to E. Right: Position-velocity diagram of feature A. The remarkable linear structure both in space and LOS velocity strongly suggests rotation seen edge-on.

$$\tau(\theta, v) = \tau_0 \int \eta(\rho) exp\left[-\frac{1}{2}\left(\frac{v - \Omega(\rho)\theta}{\Delta v_D}\right)^2\right]\frac{d\rho}{\beta} \qquad \left(\beta = \sqrt{1-(\theta/\rho)^2}\right)$$

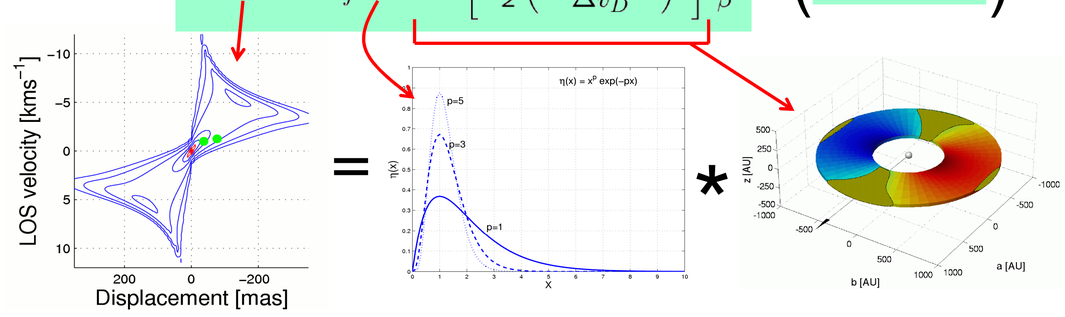

Figure 6: The optical depth $\tau(\theta,,v)$ is modelled as the velocity coherent path length (obtained by the exponential) weighted by the distribution profile of the masing material η. The free parameters are the rotational velocity at the reference radius, the index p of η and the index describing the rotation curve. We find that the rotation curve for disc in NGC7538 IRS1 N is well modelled by Keplerian rotation. The red contours in the τ-map (left) correspond to the extent of bulk of the data shown in Fig. 6. The green dots are the outliers at displacements 35 and 80mas.

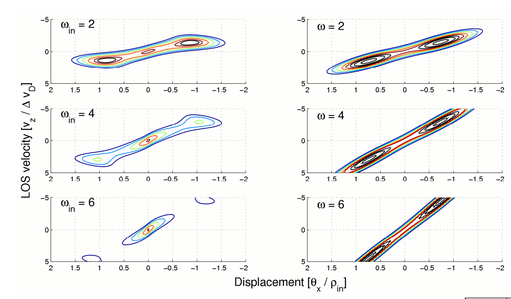

Figure 7: Comparison of position-velocity diagrams for Keplerian dynamics (left) and solid body rotation (right). The latter is not able to reproduce a maximum in the centre, while a (fast enough) Keplerian rotation is. From top to bottom the rotation velocity at the reference radius increases from twice the linewidth to 6 times the linewidth. Contours are normalised to the value at (0,0). Back contours indicate values of τ larger than 1.

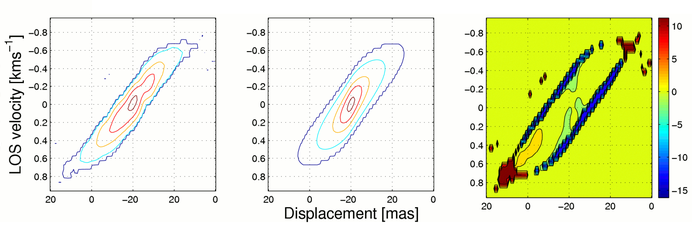

Figure 8: left: data, middle: model, right: difference. Notice that the model was calculated with three free parameters only. Such high accuracy with such a simple model is the strength of the present work.